A platinum(II) molecular hinge with motions visualized by phosphorescence changes

Yeye Ai[a,b], Michael Ho-Yeung Chan[b], Alan Kwun-Wa Chan[b], Maggie Ng[b], Yongguang Li[a,1], and Vivian Wing-Wah Yam[a,b,1]

[a]Lehn Institute of Functional Materials, School of Chemistry, Sun Yat-Sen University, Guangzhou 510275, People's Republic of China; and [b]Institute of Molecular Functional Materials (Areas of Excellence Scheme, University Grants Committee, Hong Kong) and Department of Chemistry, The University of Hong Kong, Hong Kong, People's Republic of China

Contributed by Vivian Wing-Wah Yam, May 26, 2019 (sent for review May 9, 2019; reviewed by Harry B. Gray and Peter J. Stang)

With the rapidly growing exploration of artificial molecular machines and their applications, there is a strong demand to develop molecular machines that can have their motional states and configuration/conformation changes detectable by more sensitive and innovative methods. A visual artificial molecular hinge with phosphorescence behavior changes is designed and synthesized using square-planar cyclometalated platinum(II) complex and rigid aromatic alkynyl groups as the building blocks to construct the wings/flaps and axis, respectively. The molecular motions of this single molecular hinge and its reversible processes can be powered by both solvent and temperature changes. The rotary motion can be conveniently observed by the visual phosphorescence changes from deep-red to green emission in real time.

platinum | self-assembly | luminescence

Dynamic control of movements in artificial molecular machines at the nanoscale, including rotors, motors, hinges, elevators, and shuttles, can result in electronic, photophysical, catalytic, and transport property changes (1–10), which can lead to their applications in the fields of chemistry, materials science, and biology (1, 5, 11–18). The development of convenient detection methods to monitor the molecular motions with property changes that can be observable at the macroscopic level is a major challenge (19, 20). Luminescence changes are attractive optical readouts, which can be readily monitored spectrophotometrically (4, 21–23). However, molecular machines with visual emissive color changes are rarely explored. Therefore, it is of great importance to develop molecular machines that can have their motional states and configuration/conformation changes detectable by more sensitive and convenient methods.

Emissive transition metal complexes have distinctive advantages for the construction of molecular devices with visually detectable luminescence changes due to their intrinsic ability to possess long-lived phosphorescence (24). For example, square-planar platinum(II) complexes with π-conjugated ligands can show distinctive spectroscopic properties by modulation of their aggregation and deaggregation states (25–31). Based on an understanding of the relationship between the rich phosphorescence behaviors and molecular structures, an artificial molecular hinge with platinum(II) phosphor as building blocks of the hinge wings or flaps has been designed and synthesized in this work. The rather rigid molecular hinge wings or flaps can be opened or closed by rotary motion about the central rigid axis, leading to the modulation of intramolecular distances between these planar wings or flaps. The rotary motion of this single molecular hinge can be driven and controlled reversibly by external stimuli and can be conveniently visualized as phosphorescence changes between deep-red and green emission (Fig. 1).

Results and Discussion

Dinuclear complexes **1**–**3**, together with their mononuclear control complexes **4**–**6**, were prepared by the reaction of chloroplatinum(II) precursors with their corresponding organic alkynes in the presence of NaOH in methanol (Fig. 2 and *SI Appendix*, Schemes S1 and S2). The synthetic routes, detailed procedures, and characterization data of all of the synthesized compounds are described in *SI Appendix*.

The closed hinge-like structures of the dinuclear complexes are established by the crystal structure of **2**, which reveals a closed hinge-like intramolecular staggered conformation, stabilized by intramolecular π–π interaction with an interplanar distance of about 3.4 Å (Fig. 3 and *SI Appendix*, Fig. S1). The Pt···Pt distance of 4.108 Å indicates insignificant Pt····Pt interaction. The crystal packing of **2** also suggests the lack of intermolecular π–π stacking between molecules. The crystal data, selected bond lengths, and angles are summarized in *SI Appendix*, Tables S1 and S2.

The hinge molecule **1**, with four flexible alkyl chains, shows good solubility in dichloromethane. Interestingly, a dilute solution of **1** gives a deep-red emission band at 690 nm with a high photoluminescence quantum yield of 0.56 and an emissive lifetime of 1.4 μs. The red emission exists in both dilute and concentrated solutions (6.0×10^{-6} to 2.0×10^{-3} M, *SI Appendix*, Fig. S2) with a growth of intensity upon increasing concentration. Complex **2**, without the flexible chains, also gives a deep-red

Significance

With the current interest in the development of innovative artificial machineries and robotics at the molecular and nanoscale, there is an increasing demand for the strategic design of smart machineries that can have their motional states powered by subtle environmental changes and detectable by optical readout. Through an understanding of the relationship between the intriguing phosphorescence behaviors and molecular structures, an artificial platinum(II) molecular hinge with motions associated with visually appealing phosphorescence changes has been built, which can be opened or closed by rotary motion to give drastic phosphorescence color switching. Reversible motional switching has been demonstrated to be driven by solvent/temperature changes, paving the way to the development of a simple and efficient method for visualizing molecular motion.

Author contributions: V.W.-W.Y. and Y.L. designed research; Y.A., M.H.-Y.C., A.K.-W.C., M.N., and Y.L. performed research; Y.A., M.H.-Y.C., A.K.-W.C., M.N., Y.L., and V.W.-W.Y. analyzed data; and Y.A., M.H.-Y.C., A.K.-W.C., M.N., Y.L., and V.W.-W.Y. wrote the paper.

Reviewers: H.B.G., California Institute of Technology; and P.J.S., University of Utah.

The authors declare no conflict of interest.

Data deposition: The X-ray crystallographic data have been deposited in the Cambridge Crystallographic Data Centre (CCDC), https://www.ccdc.cam.ac.uk/structures/ (CCDC reference no. 1893903).

[1]To whom correspondence may be addressed. Email: liyongguang@mail.sysu.edu.cn or wwyam@hku.hk.

This article contains supporting information online at www.pnas.org/lookup/suppl/doi:10.1073/pnas.1908034116/-/DCSupplemental.

Published online June 26, 2019.

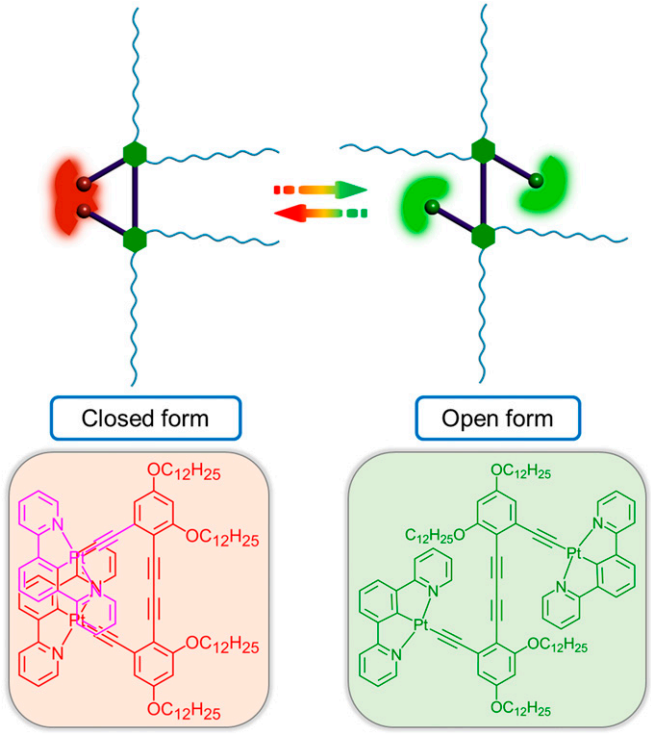

Fig. 1. Schematic representation of the rotary motion of molecular hinge.

emission at 700 nm in dilute dichloromethane solution. Similarly, the more sterically bulky complex **3** shows a red emission, slightly blue-shifted from **1** and **2** at 676 nm. The red emissions observed in the dinuclear complexes **1**–**3**, quite different from the green emission typical of the mononuclear complexes **4**–**6**, are suggestive of the retention of their closed hinge-like structures in the solution state (*SI Appendix*, Figs. S2 and S3). The insignificant changes in emission energies with concentration (*SI Appendix*, Fig. S2*A*), together with the absence of scattering signals in the dynamic light scattering (DLS) studies as well as the agreement of the UV-vis absorption bands with the Beer's law (*SI Appendix*, Fig. S2 *B* and *C*) of **1** in dichloromethane solution, suggest the absence of intermolecular aggregate formation of **1** in dichloromethane. Based on the comparison with the photophysical data of the alkynyl ligand (**L1**) and the cyclometalated mononuclear platinum complex **6** (*SI Appendix*, Fig. S2*E*), together with the X-ray crystal structures of **2**, the deep-red emission band is tentatively assigned as originating from the intramolecular ground-state π-stacking interactions in the closed hinge molecules (32, 33). These results are in line with the molecular wings or flaps being close to each other in dichloromethane solution with the formation of intramolecular π–π stacking interaction, resulting in the closed form of the molecular hinge with deep-red color emission. By density-functional theory calculations, the structures of the open and closed forms of molecular hinge **1** have been optimized with the M06 functional in dichloromethane, and their optimized geometries are shown in *SI Appendix*, Fig. S3. For the closed form of **1**, the Pt···Pt distance was computed to be 4.22 Å, which is close to the experimental value of 4.108 Å in the X-ray crystal structure of **2** (*SI Appendix*, Fig. S4), indicating that there is no significant Pt···Pt interaction. The interplanar distance of the two [Pt(N^C^N)] [N^C^N = 1,3-di(2-pyridyl)benzene (dpyb)] coordination planes has been computed to be ∼3.4 Å, which is in good agreement with the value in the X-ray crystal structure of **2**, and this indicates the presence of short π–π contacts, probably resulting from π–π interaction. In dichloromethane, the closed form of **1** is found to be more stable than the open form by a free energy of 4.24 kcal mol^{-1}, which is consistent with the experimental results, resulting from the presence of intramolecular π–π interaction in the closed form. Attempts to convert the closed hinge-like conformations to their open forms in dichloromethane by heating to 311 K lead to insignificant changes in both the absorbance and the emission energies (*SI Appendix*, Fig. S2*D*), further establishing the stability and the retention of the closed form in dichloromethane solutions. The ground-state geometries of the open and closed form of **3** have also been optimized. Shown in *SI Appendix*, Fig. S5 are the optimized structures of the open and closed forms of **3**. The interplanar distance of the two platinum(II)-ligand moiety coordination planes in the closed form of **3** is ∼3.4 Å, whereas the Pt···Pt distance is computed to be 4.28 Å. This indicates that the introduction of sterically bulky *tert*-butyl groups at 4′- and 4′′-positions and $-CF_3$ group at 4-position to the ligand moiety does not have significant effect on the intramolecular π–π interaction in the closed form, as the interplanar distances of the two platinum(II)-ligand moiety coordination planes are almost the same at ∼3.4 Å in the closed forms of **1** and **3**. The slightly blue-shifted emission band at 676 nm of **3** might indicate a possible weakening of the intramolecular π–π interaction due to the sterically bulky *tert*-butyl groups. However, the possibility of a destabilized π* orbital

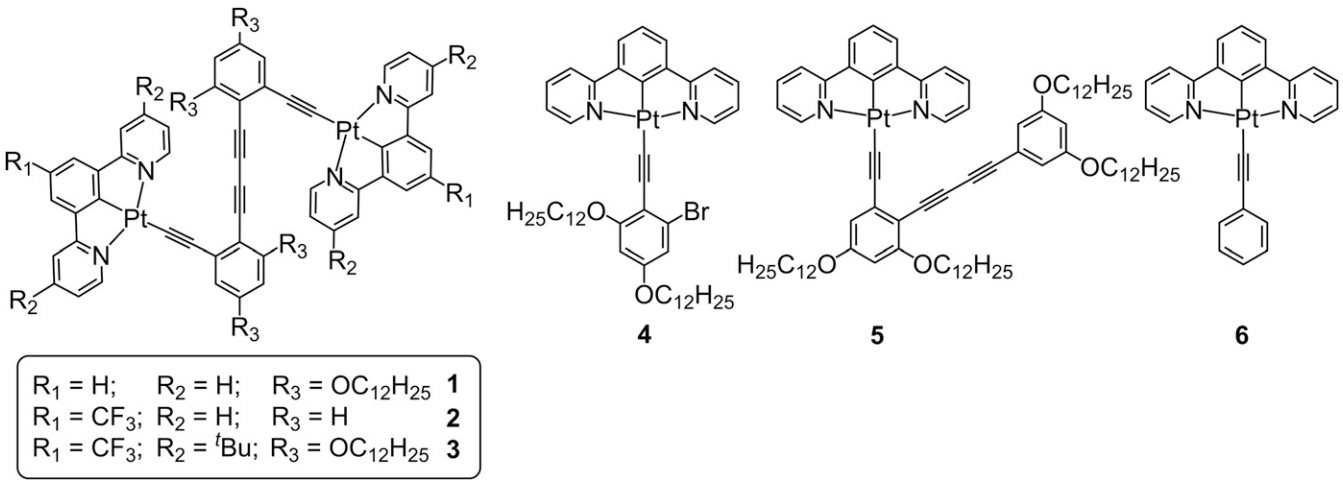

Fig. 2. Molecular structures of complexes **1**–**6**.

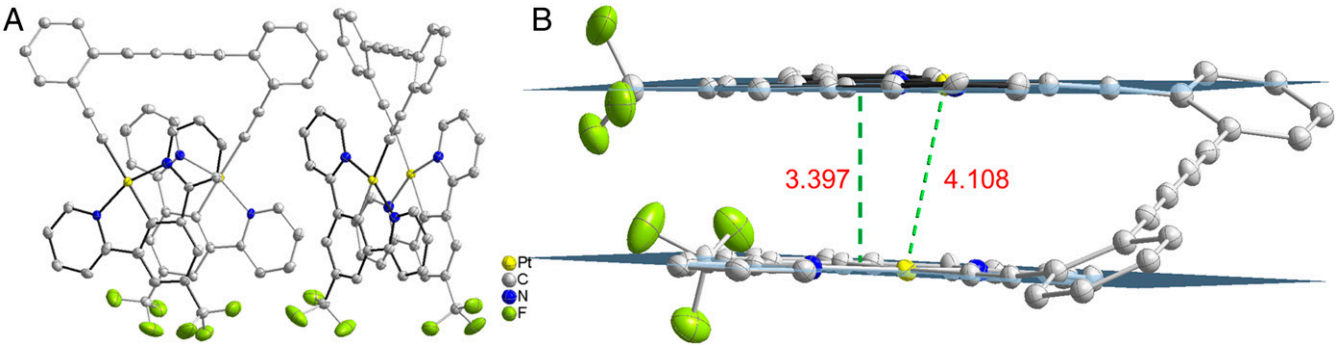

Fig. 3. (*A*) X-ray crystal structure of **2**. Hydrogen atoms are omitted for clarity. (*B*) Crystal structure of complex **2** showing the intramolecular π–π stacking interaction with interplanar distance of about 3.4 Å and Pt•••Pt distance of 4.108 Å.

of the N^C^N ligand due to the electronic effect of the more electron-donating *tert*-butyl groups cannot be excluded.

The use of the butadiynyl linker as the rigid axis capable of rotation, together with the incorporation of the square-planar cyclometalated platinum(II) moieties as wings or flaps capable of forming π–π stacking interaction, have led to the stabilization of the molecular hinge in the closed form. Given the tightness of the hinge in the closed form in dichloromethane, attempts have been made to effect the opening and closing of the molecular hinge through the control of solvation brought about by changes in the solvent compositions. Upon the addition of nonpolar poor solvents such as hexane or cyclohexane to the above dichloromethane solutions, the emission band at 690 nm shows a drop in intensity, initially accompanied by a slight red shift, followed by the almost complete disappearance of the red emission band with the concomitant appearance of a high-energy emission band at 516 nm, with the emission color showing continuous changes and finally giving a green emission (Fig. 4 and *SI Appendix*, Fig. S6). The emission energy and spectral shape of the green emission band at 516 nm are similar to that of the cyclometalated mononuclear platinum complex, [Pt(N^C^N)(C≡CPh)] (**6**) (*SI Appendix*, Fig. S7). The vibronic emission is typical of a triplet intraligand (^{3}IL) excited state (34, 35) although the possibility of a mixing of an IL excimeric emission into the ^{3}IL origin cannot be completely excluded given the absence of a well-resolved vibronic structure together with the presence of a broad tail for the green emission band. Additionally, in dilute dichloromethane solution, the control mononuclear platinum(II) complexes **4** and **5**, without the ability to form inter- or intramolecular π–π contacts, have been found to show similar green emission bands at 520 and 537 nm, respectively (*SI Appendix*, Fig. S7), suggesting the green emission in the dinuclear complexes **1** and **2** is originating from ^{3}IL emission typical of mononuclear platinum(II) analogs (34, 36). This has further been corroborated by the calculated emission wavelength maximum of 567 nm for the open form of **1**, which has been approximated by the energy difference between the ground state and the T_1 state at their corresponding optimized geometries (*SI Appendix*, Tables S3 and S7), which is close to the experimental value of 516 nm. The initial slight red shift of the red emission band indicates that the molecular hinge initially shows a tightening of the molecular wings or flaps within the closed form with reduced solvation and/or possible intermolecular aggregation. Further increase of the content of nonpolar solvent eventually leads to the transformation to the open form by the rotation of molecular wings or flaps away from each other to form the open form with the disappearance of the intramolecular π–π interaction (Fig. 1), leading to the green emission, typical of the monomeric ^{3}IL emission (Fig. 4). As shown in Movies S1 and S2, the rotational process of the molecular hinge can also be conveniently monitored by the naked eye with obvious color changes under UV light irradiation. The excitation spectrum of the emission band at λ = 690 nm (closed form) shows the presence of ground-state aggregation compared with that of the emission band at λ = 516 nm (open form) due to the intramolecular π–π stacking in the closed form as opposed to the monomeric ^{3}IL emission of the open form (*SI Appendix*, Fig. S8). The different emission origins of the 690-nm (closed form) and the 516-nm (open-form) bands have been further supported by their different emission lifetimes, as revealed from the different time-resolved emission spectra (*SI Appendix*, Fig. S10).

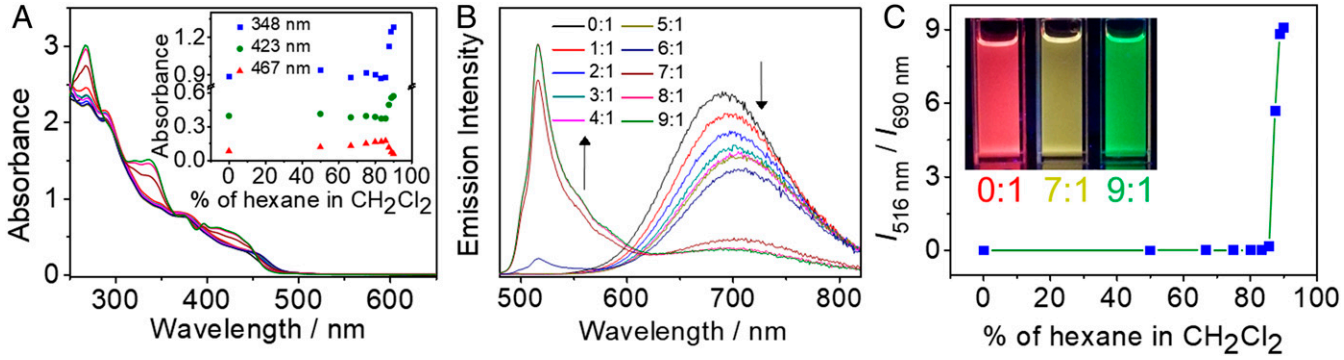

Fig. 4. Solvent-dependent (*A*) UV-vis absorption and (*B*) emission spectra of **1** upon increasing hexane portion in dichloromethane (vol/vol, 2.7×10^{-5} M). (*A, Inset*) Plots of absorbance at 348, 423, and 467 nm upon increasing hexane content. (*C*) A plot of phosphorescence intensity ratio between 516 and 690 nm (I_{516}/I_{690}) upon increasing hexane portion in dichloromethane (vol/vol, 2.7×10^{-5} M). (*Inset*) Photographs of different emission colors in hexane–dichloromethane (0:1, 7:1, 9:1, vol/vol) mixtures.

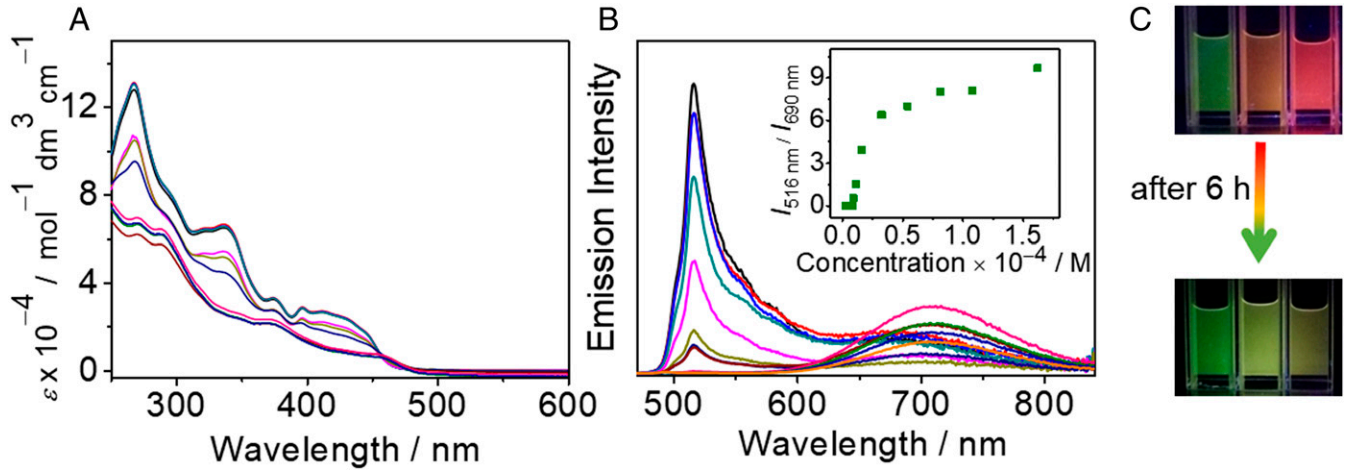

Fig. 5. Concentration-dependent (*A*) UV-vis absorption and (*B*) emission spectra of **1** in hexane–dichloromethane (9:1, vol/vol) mixtures at different concentrations from 2.0×10^{-6} to 1.3×10^{-4} M at room temperature. (*Inset*) A plot of the corresponding phosphorescence intensity ratio between 516 and 690 nm (I_{516}/I_{690}) in hexane–dichloromethane (9:1, vol/vol) mixtures at different concentrations. (*C*) Photographs of emission color changes in hexane–dichloromethane (9:1, vol/vol) mixtures at concentrations of 1.1×10^{-5}, 9.0×10^{-6}, and 4.0×10^{-6} M (from left to right).

The ease of opening or closing of the molecular hinge is affected by the different ratios of the mixed solvents. This can be monitored by following both the visual phosphorescence color and emission spectral changes. The phosphorescence color changes are found to be insignificant before the volume ratios of hexane–dichloromethane and cyclohexane–dichloromethane reach 6:1 (vol/vol) and 8:1 (vol/vol) at concentrations of 5.6×10^{-5} and 2.7×10^{-5} M, respectively. As the volume ratios reach 6:1 (vol/vol) and 8:1 (vol/vol), respectively, an abrupt change in emission color is observed with increasing contribution from the emission band at 516 nm, as shown in Fig. 4C and *SI Appendix*, Fig. S6*C*. More interestingly, the changes of emission color from deep-red to green at hexane–dichloromethane (9:1, vol/vol) and cyclohexane–dichloromethane (9:1, vol/vol) have been found to be time-dependent. Such changes in emission have been found to be dependent on the respective hexane and cyclohexane content as well as the concentration of the complex in dichloromethane solution. With a higher content of nonpolar solvents (hexane/cyclohexane) and higher concentration of the complex, the growth of the green emission is found to level off at a shorter period of time (Fig. 5 and *SI Appendix*, Fig. S11). On the other hand, the emission color changes still remain incomplete after 6 h under dilute concentrations of below 1.0×10^{-5} and 5.0×10^{-5} M for the hexane–dichloromethane (9:1, vol/vol) and cyclohexane–dichloromethane (9:1, vol/vol) mixtures, respectively (Fig. 5C and *SI Appendix*, Fig. S11*C*). Consequently, the opening and closing of the molecular hinge can be modulated by solvent and be adjusted through concentration changes.

Additionally, different nonpolar solvents have been found to influence the opening and closing processes of the molecular hinge. Cyclohexane (viscosity, $\eta = 0.984$ cP), *n*-hexane ($\eta = 0.326$ cP), *n*-decane ($\eta = 0.920$ cP), and methylcyclohexane ($\eta = 0.670$ cP) have been used to investigate the influence of solvent structure and viscosity (η) on the conversion between the open and closed forms of the molecular hinge, respectively. As shown in *SI Appendix*, Fig. S12, the time-dependent emission spectral changes in *n*-hexane–dichloromethane (9:1, vol/vol), *n*-decane–dichloromethane (9:1, vol/vol), methylcyclohexane–dichloromethane (9:1, vol/vol), and cyclohexane–dichloromethane (9:1, vol/vol) mixtures (5.4×10^{-5} M) attain a level off of the emission intensity in about 7.5, 7.5, 13, and 21 min, respectively, under ambient conditions. In general, the *n*-alkane–dichloromethane mixtures require shorter time than the cycloalkane–dichloromethane mixtures in the transformation process. This observation might be attributed to the greater steric effect imposed by cyclohexane and methylcyclohexane that would hinder the hydrophobic interaction of the long alkyl chains on the complex, different from the straight-chain zig-zag-structures of *n*-hexane and *n*-decane, resulting in a longer time for such emission spectral changes to attain equilibrium. Although the addition of *n*-hexane and *n*-decane to the dichloromethane solutions take similar time to achieve the phosphorescence color changes, the methylcyclohexane–dichloromethane mixture requires shorter time than the cyclohexane–dichloromethane mixture. It is likely that viscosity also plays a role in their differences despite the similar structure and the similar steric environment of methylcyclohexane and cyclohexane. Such results indicate that both the structure and viscosity of the poor solvent molecules can influence the opening and closing processes of the molecular hinge, which is more prominent in the sterically crowded environment. A qualitative energy landscape diagram has been proposed to illustrate the conversion processes (Fig. 6). Despite the less stable conformation of the open form than the closed form in good solvents such as dichloromethane, the reduced solvation, brought about by the addition of a poor solvent, can provide the driving force for the molecular rotation to the open form through formation of intermolecular aggregates of the open form, stabilized by π–π stacking interactions (*vide infra*). Interestingly, the rather loose packing of the π-stacked open-form

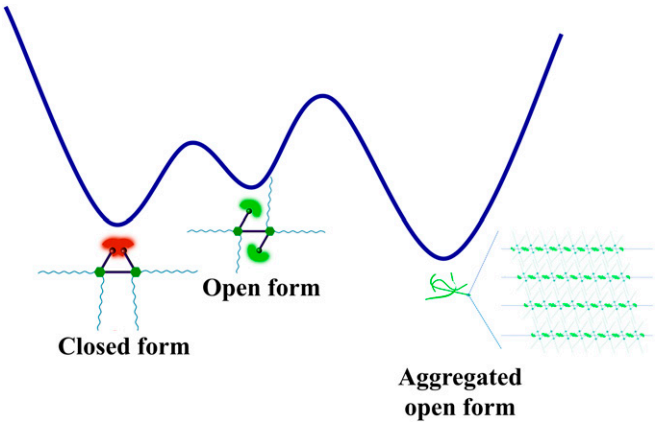

Fig. 6. A qualitative energy landscape diagram.

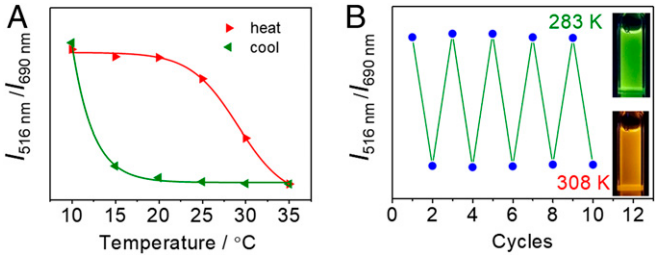

Fig. 7. (*A*) Temperature-dependent phosphorescence intensity ratio between 516 and 690 nm of molecular hinge **1** in cyclohexane–dichloromethane (9:1, vol/vol) mixture (5.6×10^{-5} M) with heating and cooling processes; (*B*) Reversible process of the molecular hinge rotation with phosphorescence intensity ratio between 516 and 690 nm (I_{516}/I_{690}) in cyclohexane–dichloromethane (9:1, vol/vol) mixture (5.6×10^{-5} M) in five cycles. (*Inset*) Photographs of cyclohexane-dichloromethane (9:1, vol/vol) mixture at 283 K (*Top*) and 308 K (*Bottom*).

aggregates is already sufficient to provide the stabilization to facilitate the opening of the molecular hinge.

More interestingly, the reversed molecular motion is able to be controlled by temperature. After the formation of the open form of the molecular hinge in the mixed solvents at a relatively low temperature, it can revert back to the closed form upon increasing the temperature (Fig. 7 and *SI Appendix*, Figs. S13 and S14). In the process of heating, due to the disruption of the loosely packed intermolecular aggregates, the intramolecular π−π stacking interactions could become dominant again by molecular wings or flaps rotating back to the closed form to stabilize the molecules, which is in line with the visual phosphorescence color changes from green to red (Fig. 7). The reversibility of such opening/closing processes has been investigated by UV-vis and emission spectroscopy (Fig. 7 and *SI Appendix*, Fig. S14), as well as can be observed by the naked eye. Notably, reversible changes of the emission color of five successive cycles have been observed, suggesting the manipulation of the molecular hinge motions by temperature. The concentration-dependent and temperature-dependent UV-vis kinetic traces at 425 nm of **1** in hexane–dichloromethane (9:1, vol/vol) and cyclohexane–dichloromethane (9:1, vol/vol) mixtures have also been recorded and shown in *SI Appendix*, Figs. S15 and S16.

In contrast to the closed form, in which no aggregates are formed in dichloromethane, molecular association has been observed in the open form in hexane–dichloromethane (9:1, vol/vol) and cyclohexane–dichloromethane (9:1, vol/vol) mixtures, as revealed from the DLS studies (*SI Appendix*, Fig. S17). In addition, the originally well-resolved proton signals in the ^{1}H NMR experiments in CD_2Cl_2 disappear as the proportion of hexane-d_{14} increases to 90%, further suggesting the formation of aggregates in the open form (*SI Appendix*, Fig. S18). One-dimensional nanowires are observed in the TEM and SEM images prepared from samples of hexane–dichloromethane (9:1, vol/vol) and cyclohexane–dichloromethane (9:1, vol/vol) mixtures. The nanowires are estimated to be about 2.0 nm thick according to the AFM images (Fig. 8 and *SI Appendix*, Fig. S19). A ratio of about 1:1/2:1/3:1/4:1/5 is observed in the XRD patterns, indicating the possible formation of lamellar packing for the molecules with corresponding *d* spacing of about 33.8 Å (*SI Appendix*, Fig. S20). Upon the addition of nonpolar solvents, the observation of phosphorescence color changes from deep-red to green suggests that the molecular hinge wings are isolated and are rotated far away from each other to the open form. These, together with results from DLS studies, suggest that the open-form molecules would tend to aggregate together to minimize the energy with the formation of one-dimensional nanowires in hexane–dichloromethane (9:1, vol/vol) and cyclohexane–dichloromethane (9:1, vol/vol) mixtures, probably in a fairly loose manner, as revealed by the lack of low-energy emission bands. The alkyl chains are well-dispersed and would orient themselves toward hexane/cyclohexane to stabilize the one-dimensional nanowire. Therefore, the open form of the molecular hinge could be stabilized with the formation of aggregates. A possible structural model for the one-dimensional nanofiber is proposed in *SI Appendix*, Fig. S21. Further investigation on the aggregation properties of complex **3** in hexane–dichloromethane mixture (9:1, vol/vol) has been performed. However, no significant changes of the red emission have been observed upon addition of hexane into the dichloromethane solution of **3**. In fact, **3** shows very good solubility in hexane as well as in other relatively nonpolar solvents such as cyclohexane, benzene, and toluene. This could be attributed to the lack of driving forces in the formation of aggregates from the open form of **3** and thus no opening/closing processes could be observed. From the above results, the formation of open-form aggregates is believed to provide sufficient driving force to facilitate the opening of the molecular hinge. These suggest the importance on the molecular design that leads to the opening/closing of the molecular hinge, representing a special kind of functionality.

In summary, an artificial molecular hinge with molecular motions detectable by phosphorescence behavior changes has been designed and constructed. In this single molecular hinge, square-planar cyclometalated platinum(II) complex with rigid aromatic alkynyl groups are used as the building blocks to construct the wings

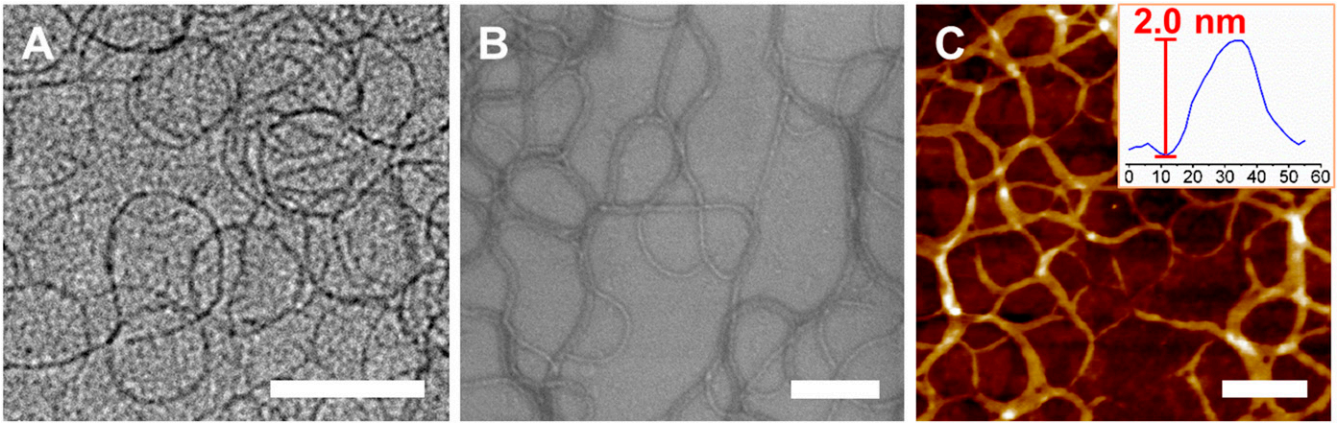

Fig. 8. (*A*) TEM, (*B*) SEM, and (*C*) AFM images of molecular hinge **1** prepared from hexane–dichloromethane mixture (9:1, vol/vol) (5.6×10^{-5} M) (Scale bars, 200 nm.)

or flaps and axis of the molecular hinge, respectively. Drastic phosphorescence color changes (between green and deep-red emission) are observed during the molecular motions between open and closed form. The reversible motional changes of this monomolecular hinge can be realized, as driven by solvent and temperature changes. Based on the visual phosphorescence changes, the different states of the molecular hinge between open form and closed form can be conveniently regulated and observed by the naked eye.

Materials and Methods

The chloroplatinum(II) precursors were prepared by the reaction of $K_2[PtCl_4]$ with the corresponding cyclometalating ligands in glacial acetic acid. Dinuclear alkynylplatinum(II) complexes **1**–**3**, together with their mononuclear control complexes **4**–**6**, were prepared by the reaction of chloroplatinum(II) precursors with their corresponding organic alkynes in the presence of NaOH in methanol. The detailed procedures and characterization of all of the synthesized compounds are described in *SI Appendix*.

See *SI Appendix* for the following: Experimental section; Physical Measurements and Instrumentations; Crystal structure and determination data (CCDC 1893903); Computational Details; Solvent- and time-dependent UV-vis and emission spectra (PDF); X-ray crystallographic data for Complex **2** (CIF); Movie S1, showing the luminescence changes in hexane–dichloromethane mixture of **1** (AVI), and Movie S2, showing the luminescence changes in cyclohexane–dichloromethane mixture of **1** (AVI).

ACKNOWLEDGMENTS. This work was supported by the National Natural Science Foundation of China (21871297 and 21503284), the Fundamental Research Funds for the Central Universities (17lgpy77), the University Grants Committee Areas of Excellence (AoE) Scheme (AoE/P-03/08), and a General Research Fund grant from the Research Grants Council of the Hong Kong Special Administrative Region, People's Republic of China (HKU 17302918). V.W.-W.Y. acknowledges support from the University of Hong Kong under the University Research Committee (URC) Strategically Oriented Research Theme on Functional Materials for Molecular Electronics and the Sun Yat-Sen University. Dr. Jing Guo in the Department of Chemistry, Sun Yat-Sen University, is gratefully acknowledged for X-ray data collection and solving the crystallographic data. The computations were performed using the research computing facilities provided by Information Technology Services, The University of Hong Kong.

1. M. Xue, Y. Yang, X. Chi, X. Yan, F. Huang, Development of pseudorotaxanes and rotaxanes: From synthesis to stimuli-responsive motions to applications. *Chem. Rev.* **115**, 7398–7501 (2015).
2. M. R. Wilson *et al*., An autonomous chemically fuelled small-molecule motor. *Nature* **534**, 235–240 (2016).
3. E. R. Kay, D. A. Leigh, F. Zerbetto, Synthetic molecular motors and mechanical machines. *Angew. Chem. Int. Ed. Engl.* **46**, 72–191 (2007).
4. M. Cheng *et al*., Acid/base-controllable fluorescent molecular switches based on cryptands and basic N-heteroaromatics. *Chem. Commun. (Camb.)* **53**, 11838–11841 (2017).
5. K. Zhu, G. Baggi, S. J. Loeb, Ring-through-ring molecular shuttling in a saturated [3] rotaxane. *Nat. Chem.* **10**, 625–630 (2018).
6. F. Durola, J. Rebek, Jr, The ouroborand: A cavitand with a coordination-driven switching device. *Angew. Chem. Int. Ed. Engl.* **49**, 3189–3191 (2010).
7. A. D. Hamilton, D. Van Engen, Induced fit in synthetic receptors: Nucleotide base recognition by a molecular hinge. *J. Am. Chem. Soc.* **109**, 5035–5036 (1987).
8. S. A. Nagamani, Y. Norikane, N. Tamaoki, Photoinduced hinge-like molecular motion: Studies on xanthene-based cyclic azobenzene dimers. *J. Org. Chem.* **70**, 9304–9313 (2005).
9. S. K. Samanta, D. Samanta, J. W. Bats, M. Schmittel, DABCO as a dynamic hinge between cofacial porphyrin panels and its tumbling inside a supramolecular cavity. *J. Org. Chem.* **76**, 7466–7473 (2011).
10. R. Nandy, M. Subramoni, B. Varghese, S. Sankararaman, Intramolecular π-stacking interaction in a rigid molecular hinge substituted with 1-(pyrenylethynyl) units. *J. Org. Chem.* **72**, 938–944 (2007).
11. H. Wu, Y. Chen, Y. Liu, Reversibly photoswitchable supramolecular assembly and its application as a photoerasable fluorescent ink. *Adv. Mater.* **29**, 1605271 (2017).
12. Y. Cheng *et al*., Multiscale humidity visualization by environmentally sensitive fluorescent molecular rotors. *Adv. Mater.* **29**, 1703900 (2017).
13. Q.-W. Zhang *et al*., Multicolor photoluminescence including white-light emission by a single host-guest complex. *J. Am. Chem. Soc.* **138**, 13541–13550 (2016).
14. W. Yang, Y. Li, H. Liu, L. Chi, Y. Li, Design and assembly of rotaxane-based molecular switches and machines. *Small* **8**, 504–516 (2012).
15. V. Blanco, D. A. Leigh, V. Marcos, Artificial switchable catalysts. *Chem. Soc. Rev.* **44**, 5341–5370 (2015).
16. N. Mittal, S. Pramanik, I. Paul, S. De, M. Schmittel, Networking nanoswitches for ON/OFF control of catalysis. *J. Am. Chem. Soc.* **139**, 4270–4273 (2017).
17. D. P. Iwaniuk, C. Wolf, A stereodynamic probe providing a chiroptical response to substrate-controlled induction of an axially chiral arylacetylene framework. *J. Am. Chem. Soc.* **133**, 2414–2417 (2011).
18. L. E. Franken *et al*., Solvent mixing to induce molecular motor aggregation into bowl-shaped particles: Underlying mechanism, particle nature, and application to control motor behavior. *J. Am. Chem. Soc.* **140**, 7860–7868 (2018).
19. H. Tian, Q. C. Wang, Recent progress on switchable rotaxanes. *Chem. Soc. Rev.* **35**, 361–374 (2006).
20. G. S. Kottas, L. I. Clarke, D. Horinek, J. Michl, Artificial molecular rotors. *Chem. Rev.* **105**, 1281–1376 (2005).
21. E. M. Pérez, D. T. Dryden, D. A. Leigh, G. Teobaldi, F. Zerbetto, A generic basis for some simple light-operated mechanical molecular machines. *J. Am. Chem. Soc.* **126**, 12210–12211 (2004).
22. Q. C. Wang, D. H. Qu, J. Ren, K. Chen, H. Tian, A lockable light-driven molecular shuttle with a fluorescent signal. *Angew. Chem. Int. Ed. Engl.* **43**, 2661–2665 (2004).
23. X. Ma *et al*., A room temperature phosphorescence encoding [2]rotaxane molecular shuttle. *Chem. Sci. (Camb.)* **7**, 4582–4588 (2016).
24. V. W.-W. Yam, V. K.-M. Au, S. Y.-L. Leung, Light-emitting self-assembled materials based on d^8 and d^{10} transition metal complexes. *Chem. Rev.* **115**, 7589–7728 (2015).
25. A. Aliprandi, M. Mauro, L. De Cola, Controlling and imaging biomimetic self-assembly. *Nat. Chem.* **8**, 10–15 (2016).
26. C. Po, A. Y.-Y. Tam, K. M.-C. Wong, V. W.-W. Yam, Supramolecular self-assembly of amphiphilic anionic platinum(II) complexes: A correlation between spectroscopic and morphological properties. *J. Am. Chem. Soc.* **133**, 12136–12143 (2011).
27. V. C.-H. Wong *et al*., Formation of 1D infinite chains directed by metal-metal and/or π-π stacking interactions of water-soluble platinum(II) 2,6-bis(benzimidazol-2′-yl)pyridine double complex salts. *J. Am. Chem. Soc.* **140**, 657–666 (2018).
28. S. Y.-L. Leung, K. M.-C. Wong, V. W.-W. Yam, Self-assembly of alkynylplatinum(II) terpyridine amphiphiles into nanostructures via steric control and metal-metal interactions. *Proc. Natl. Acad. Sci. U.S.A.* **113**, 2845–2850 (2016).
29. Y.-K. Tian, Y.-G. Shi, Z.-S. Yang, F. Wang, Responsive supramolecular polymers based on the bis[alkynylplatinum(II)] terpyridine molecular tweezer/arene recognition motif. *Angew. Chem. Int. Ed. Engl.* **53**, 6090–6094 (2014).
30. M. Han, Y. Tian, Z. Yuan, L. Zhu, B. Ma, A phosphorescent molecular "butterfly" that undergoes a photoinduced structural change allowing temperature sensing and white emission. *Angew. Chem. Int. Ed. Engl.* **53**, 10908–10912 (2014).
31. Y. Li *et al*., Supramolecular self-assembly and dual-switch vapochromic, vapoluminescent, and resistive memory behaviors of amphiphilic platinum(II) complexes. *J. Am. Chem. Soc.* **139**, 13858–13866 (2017).
32. Z.-L. Gong, Y.-W. Zhong, J. Yao, Regulation of intra- and intermolecular Pt–Pt and π–π interactions of a U-shaped diplatinum complex to achieve pseudo-polymorphic emissions in solution and crystalline states. *J. Mater. Chem.* **5**, 7222–7229 (2017).
33. S. Develay, J. A. G. Williams, Intramolecular excimers based on rigidly-linked platinum(II) complexes: Intense deep-red triplet luminescence in solution. *Dalton Trans.*, 4562–4564 (2008).
34. Y. Chen *et al*., Photoresponsive supramolecular organometallic nanosheets induced by Pt(II)...Pt(II) and C-H...π interactions. *Angew. Chem. Int. Ed. Engl.* **48**, 9909–9913 (2009).
35. C.-J. Lin, Y. H. Liu, S. M. Peng, T. Shinmyozu, J. S. Yang, Excimer–monomer photoluminescence mechanochromism and vapochromism of pentiptycene-containing cyclometalated platinum(II) complexes. *Inorg. Chem.* **56**, 4978–4989 (2017).
36. H. Sesolis *et al*., Dinuclear (N^C^N) pincer Pt(II) complexes with bridged organometallic linkers: Synthesis, structures, self-aggregation, and photophysical properties. *Organometallics* **36**, 4794–4801 (2017).